A first attempt at time-variable gravity recovery from CHAMP using the energy balance approach

Nico Sneeuw
University of Calgary, Department of Geomatics Engineering, sneeuw@ucalgary.ca

Christian Gerlach, Dražen Švehla
Technische Universität München, Institut für Astronomische und Physikalische Geodäsie

Christian Gruber
Technische Universität Berlin, Institut für Geodäsie und Geoinformationstechnik

Abstract. Using the principle of energy conservation has been considered for gravity field determination from satellite observations since the early satellite era. CHAMP is the first satellite to which the energy balance approach can be usefully applied, now that near-continuous orbit tracking by GPS is available, aided by accelerometry. The feasibility of this approach has recently been demonstrated.

The abundance and quality of CHAMP data should allow us to monitor the Earth's gravity field over time. In this paper we will investigate the strengths and weaknesses of the energy balance approach for purposes of time-variable gravity field recovery. The quality of the required orbit is discussed in terms of GPS data, accelerometry and orbit processing. Also the quality and the physical relevance of the output gravity field time-series will be analyzed.

Keywords. CHAMP, Jacobi integral, accelerometer calibration, time variable gravity field

1 Introduction

Using the principle of energy conservation for gravity field recovery purposes has been considered since the beginning of the satellite era (O'Keefe, 1957; Bjerhammar, 1967; Reigber, 1969). In case of a rotating Earth it is not the trivial kinetic plus potential energy that is conserved. O'Keefe (1957) used a constant of restricted three-body motion, already defined by the mathematician C. Jacobi (1804–1851), the so-called Jacobi integral.

Although the theoretical framework for gravity field recovery based on the energy approach did exist (Jekeli, 1999), a lack of continuous data has always stood in the way of practical implementation. Recently, a simulation study successfully demonstrated the feasibility of using continuous and 3D GPS-determined orbits for gravity field determination (Visser et al., 2002). The concept has now been sufficiently demonstrated with real data of the CHAMP mission, (Gerlach et al., 2002) and (Han et al., 2002). The geoids reported in these works are qualitatively equivalent to the official CHAMP geoid solution EIGEN-1S, cf. (Reigber et al., 2002).

In this paper we attempt to take this success one step further. The CHAMP rapid science orbits RSO and accelerometer data ACC of the first half of 2002 will be used to obtain a time-series of monthly gravity field solutions. Moreover, we will use reduced-dynamic orbits, calculated from GPS data. The sensitivity of the gravity field end-product with respect to the orbit determination is analyzed.

2 The Jacobi integral

The Jacobi integral is a constant of the motion in a rotating frame. Here we will use an extended version that includes dissipative forces. The derivation of the Jacobi integral starts from the equation of motion in a rotating frame (Schneider, 1992, §5.4).

$$\ddot{\boldsymbol{x}} = \boldsymbol{f} + \nabla V + \nabla Z - 2\boldsymbol{\omega} \times \dot{\boldsymbol{x}} - \dot{\boldsymbol{\omega}} \times \boldsymbol{x} \,. \quad (1)$$

The accelerations at the right hand side of (1) are dissipative force (per unit mass) $\boldsymbol{f}$, gravitational force, centrifugal, Coriolis and Euler acceleration, respectively. The gravitational and centrifugal accelerations have been written as the gradient of the gravitational potential V and the centrifugal potential $Z = \frac{1}{2}\omega^2(x^2 + y^2)$, respectively. The vectors $\boldsymbol{x}$, $\dot{\boldsymbol{x}}$ and $\ddot{\boldsymbol{x}}$ are positions, velocities and accelerations in the rotating frame. The Earth rotation $\boldsymbol{\omega}$ is assumed to be constant, such that the Euler term cancels.

If we multiply (1) by the velocity $\dot{\boldsymbol{x}}$ the part with the Coriolis acceleration will drop out:

$$\begin{aligned}\dot{\boldsymbol{x}}\cdot\ddot{\boldsymbol{x}} &= \dot{\boldsymbol{x}}\cdot\boldsymbol{f} + \dot{\boldsymbol{x}}\cdot(\nabla V + \nabla Z) \\ &= \dot{\boldsymbol{x}}\cdot\boldsymbol{f} + \frac{\mathrm{d}(V+Z)}{\mathrm{d}t} - \frac{\partial(V+Z)}{\partial t}\end{aligned} \quad (2)$$

The latter step is due to the fact that the total time derivative of a potential is written as:

$$\frac{\mathrm{d}\Phi}{\mathrm{d}t} = \frac{\partial\Phi}{\partial\boldsymbol{x}}\cdot\frac{\mathrm{d}\boldsymbol{x}}{\mathrm{d}t} + \frac{\partial\Phi}{\partial t} = \dot{\boldsymbol{x}}\cdot\nabla\Phi + \frac{\partial\Phi}{\partial t}\,.$$

Because of the constant $\boldsymbol{\omega}$ the centrifugal potential has no explicit time derivative $\partial Z/\partial t$. Thus, upon integration, we are left with:

$$\int \dot{\boldsymbol{x}}\cdot\ddot{\boldsymbol{x}}\,\mathrm{d}t = \int (\dot{\boldsymbol{x}}\cdot\boldsymbol{f} - \frac{\partial V}{\partial t})\,\mathrm{d}t + V + Z + c\,.$$

The integration constant c is called *Jacobi constant* (O'Keefe, 1957). The left hand side is the kinetic energy (per unit mass) $\frac{1}{2}\dot{\boldsymbol{x}}\cdot\dot{\boldsymbol{x}}$. The gravitational potential is split up in a normal (gravitational) part and a disturbance: $V = U + T$. Rearrangement gives:

$$T + c = E_{\mathrm{kin}} - U - Z - \int \boldsymbol{f}\cdot\mathrm{d}\boldsymbol{x} + V_t \quad (3)$$

Equation (3) is the basis for gravity field determination using the energy balance approach. At the left we have the unknown disturbing potential, up till an unknown constant. All terms at the right are determined from CHAMP data or existing models:

- E_{kin} requires orbit velocities $\dot{\boldsymbol{x}}$,
- U, the normal gravitational potential, requires satellite positions $\boldsymbol{x}$,
- Z, the centrifugal potential at the satellite's location is also calculated from $\boldsymbol{x}$,
- $\int \boldsymbol{f}\cdot\mathrm{d}\boldsymbol{x}$ is the dissipated energy, which is an integral of CHAMP's accelerometer data $\boldsymbol{f}$ along the orbit,
- V_t is the time-variable gravity potential.

V_t contains both known sources (tides, 3rd bodies), that can be corrected in (3), and unknown gravity field changes.

3 Data processing

Data. The gravity field is determined from orbital data ($\boldsymbol{x}$,$\dot{\boldsymbol{x}}$), accelerometry ($\boldsymbol{f}$) and ancillary data (attitude, tides, ...). Our main analysis will be based on Rapid Science Orbits (RSO, revision $*$.9) from GFZ Potsdam. These are reduced-dynamic orbits, based on the gravity field model GRIM5-C1 (actually based on an in-house model called `grim5.c1_chmp.000924`). We will also employ more precise Reduced-Dynamic Orbits (RDO) from TU Munich. They are zero-difference orbits, with empirical accelerations modelled as stochastic impulses, taking place every 15 minutes. Their underlying gravity field model is EIGEN-1S. The time span is January through July 2002.

A rough check on the quality of RSOs is allowed by the fact that consecutive estimates of orbital arcs have a two-hour overlap period. From fig. 1 one can deduce that orbit positions are at the dm-level, whereas orbital velocity is precise up to a few tenths of mm/s. For the more precise RDO we have accuracies of 5 cm and 0.1 mm/s, respectively. The positional accuracy comes from comparison to SLR data.

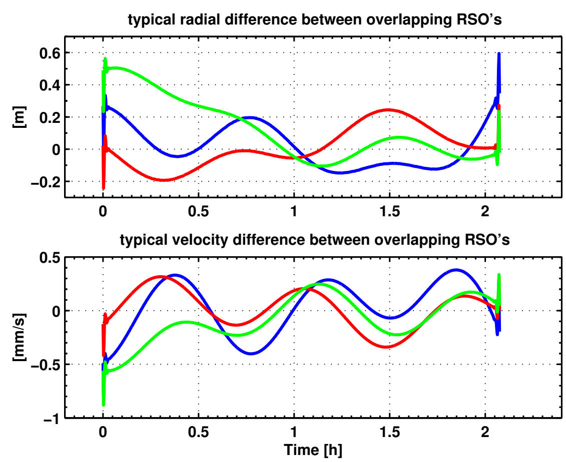

Fig. 1. Orbital accuracy can be assessed from RSO overlaps in time.

Monthly solutions. Based on pre-mission error analysis, the resolution of CHAMP's static gravity field recovery is expected to be around maximum degree $L = 75$. A Nyquist-type rule of thumb says that we need at least twice as much orbital revolutions. With the given orbital revolution rate—around 16 revolutions per day—we would need 10-day time-series. However, due to its decaying orbit CHAMP will go through several commensurabilities. A particular bad example occurred the first half of May, during which CHAMP was basically in a 31 revolutions per 2 days repeat mode, cf. fig. 2. To build in a safety margin, we made use of one month data sets. The implication is that for each individual month the gravity field is considered stationary.

The time-series of the monthly solutions should reflect the time evolution of the gravity field. Naturally, all shorter period phenomena will alias into the individual solutions. It is believed, though, that with the

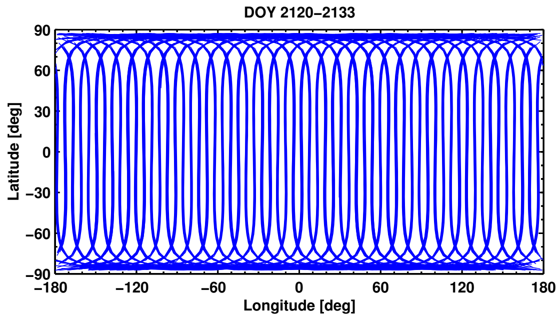

Fig. 2. Ground-track pattern during the first half of May 2002. CHAMP performed 31 revolutions in 2 days.

present accuracy of CHAMP data and orbit determination, this effect is insignificant. If necessary, a priori models should be used and the solutions iterated.

Accelerometer calibration: slope analysis vs. cross-over scheme. The CHAMP accelerometer, in particular the radial component, is known to be deficient. Moreover, accelerometers in general show a reduced performance at lower frequencies. The energy approach clearly reveals this behaviour. When ignoring the dissipative term in (3), the disturbing potential clearly drifts away from a constant level. Figure 3 shows a magnitude of the drift of about 180 $^{m^2}/_{s^2}$ per day. Obviously, energy dissipation takes place. If, however, we correct for the dissipation with raw ACC data the drift only becomes worse (2300 $^{m^2}/_{s^2}$ per day). After calibration the disturbing potential is seen to fluctuate around a constant, indeed.

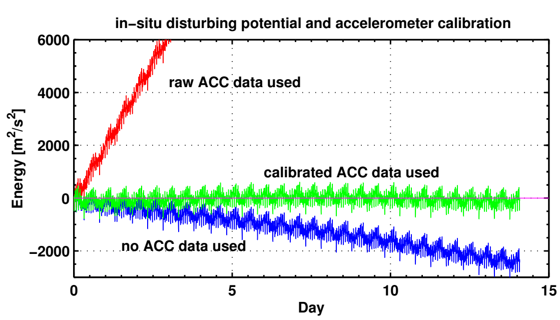

Fig. 3. Time-series of disturbing potential (up to an arbitrary constant) calculated from (3) without considering energy dissipation (lower curve), with using raw ACC (upper curve) and with calibrated ACC data (middle curve).

One way of calibrating is to compare an uncalibrated curve (e.g. figure 3, upper curve) with a corresponding time-series implied by an existing gravity field model, cf. (Han et al., 2002). The calibration consists of determining a slope between these two curves. One estimates a single bias term, which integrates to become a drift in (3). This type of calibration will be performed on the RDO that were calculated using 15-minute stochastic pulses. Thus for each 15-minute set of data a slope adjustment is performed with EIGEN-1S as reference field.

The calibration of the time-series from the RSO is performed using cross-over (XO) analysis. For each XO we have a condition that the energy level on the ascending and the descending arcs be the same. The whole set of XO constraints constitutes a powerful tool for monitoring the accelerometer behaviour. The only flaw is that the satellite arcs don't cross exactly in radial direction and that data is not available at the exact location due to discrete sampling, see fig. 4. Interpolation in both horizontal and vertical direction, using a priori knowledge, is therefore required.

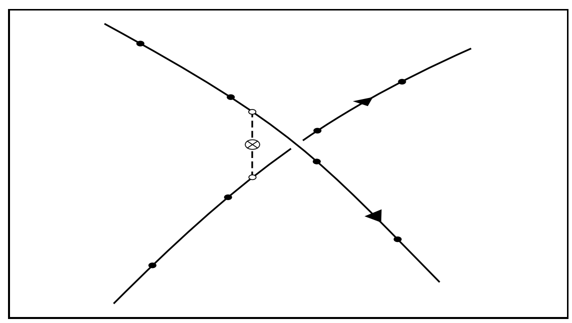

Fig. 4. Principle of creating a virtual cross-over point.

Since the cross-track dissipative forces are small, we consider only a bias and scale factor in the along-track accelerometer channel. Because these parameters are not constant in time, they are estimated daily.

Spherical harmonic analysis. Several approaches for determining spherical harmonic (SH) coefficients exist. Han et al. (2002) apply a time-wise approach with iterative brute-force inversion, which allows the use of data at their exact measurement location. Gerlach et al. (2002) employ a semi-analytical approach in which they reduce the data to a torus of constant radius, cf. (Sneeuw, 2001). Alternatively one can reduce the data to a sphere of constant radius (at satellite altitude). Here we will apply the torus approach. The data processing consists of the following steps:

- radial continuation of calibrated data onto a torus (alternatively a sphere) of constant radius,
- gridding onto equi-angular grid,
- global spherical harmonic analysis (GSHA)

using inclination functions $\bar{F}_{lmk}(I)$ (alternatively standard GSHA using spherical harmonics $\bar{Y}_{lm}(\theta, \lambda)$),

- downward continuation in the spectral domain,
- restitution of the normal field.

Clearly some approximations are involved. In particular radial continuation, using an a priori gravity field, is required for the creation of the virtual cross-overs and for the projection onto the torus (sphere). Therefore the solution needs to be iterated.

Note that the unknown Jacobi constant does not pose a problem. After GSHA the $C_{0,0}$ coefficient is simply discarded.

4 Error analysis

Let us assume our accuracy goal for the disturbing potential at satellite height is $1\,\mathrm{m^2/s^2}$. According to Bruns's equation $N = T/\gamma$ this would be equivalent to geoid accuracy—still at satellite height—of about 1 dm. The Jacobi integral (3) tells us what orbit accuracies are required, which terms can be neglected and how accurate a priori models should be. See also (Visser et al., 2002).

- The differential form of the kinetic energy reads:
$$\mathrm{d}E_{\mathrm{kin}} = \dot{\boldsymbol{x}} \cdot \mathrm{d}\dot{\boldsymbol{x}}$$
Thus, the maximum error in energy will occur for along-track velocity errors. With an orbital velocity of roughly $7\,\mathrm{km/s}$ we must require a velocity accuracy of $0.14\,\mathrm{mm/s}$. The RSO cannot meet this requirement. The RDO velocity accuracy, on the other hand, would allow sub-dm geoid recovery.
Determining velocities from orbit positions would be troublesome. Variance propagation gives: $\sigma_{\dot{x}} = \sqrt{2}\sigma_x/\Delta t$. With 10 s sampling and 1 dm orbit accuracy, one ends up with $1.4\,\mathrm{cm/s}$ velocity accuracy, two orders of magnitude worse than the requirement. In reality the propagated velocity accuracy would be less because of correlations.
- The main component of the normal potential U is the central term $GM/|\boldsymbol{x}|$. An orbit error $\mathrm{d}\boldsymbol{x}$ induces an error in the potential:
$$\mathrm{d}U = \frac{GM}{|\boldsymbol{x}|^3}\boldsymbol{x} \cdot \mathrm{d}\boldsymbol{x} = \gamma\,\mathrm{d}r$$
i.e. the radial orbit error times normal gravity (at satellite height), which is Bruns's equation in disguise. This leads to an orbit error requirement of 1 dm. This is at the edge of the RSO accuracy.
- An orbit error causes the centrifugal potential Z to be off by:
$$\mathrm{d}Z = (\boldsymbol{\omega} \times \boldsymbol{x}) \cdot (\boldsymbol{\omega} \times \mathrm{d}\boldsymbol{x}) = \omega^2 (x\,\mathrm{d}x + y\,\mathrm{d}y)$$
This would lead to a more relaxed orbit requirement of several meters.
- We assumed the rotation axis to be constant in size and direction. The effect of an orientation perturbation $\mathrm{d}\boldsymbol{\omega}$ on Z would be:
$$\mathrm{d}Z = (\boldsymbol{\omega} \times \boldsymbol{x}) \cdot (\mathrm{d}\boldsymbol{\omega} \times \boldsymbol{x})$$
which is basically the formula for pole tide at satellite altitude. Due to polar motion, the true rotation axis is $\omega[x_{\mathrm{P}}\ -y_{\mathrm{p}}\ 1]^{\mathsf{T}}$, so that $\mathrm{d}\boldsymbol{\omega} = \omega[x_{\mathrm{P}}\ -y_{\mathrm{P}}\ 0]^{\mathsf{T}}$. Inserting a typical polar motion magnitude of $0\overset{''}{.}3$ roughly leads to a potential error of only $\mathrm{d}Z \approx \pm 0.2\,\mathrm{m^2/s^2}$. Moreover, a time-variable rotation vector $\boldsymbol{\omega}$ would require additional Euler terms in the equation of motion (1) and in the Jacobi integral (3).
- It is assumed that the calibration of ACC data can be controlled with sufficient precision to guarantee an error in the dissipated energy below $1\,\mathrm{m^2/s^2}$.
- The explicitly time-variable potential V_t is comprised of many components. The direct astronomical tidal potential, which may fluctuate $\pm 3\,\mathrm{m^2/s^2}$ can be modelled accurately. The known portion of solid Earth and ocean tides is modelled well enough to leave the residuals below our goals.

Moreover, approximation errors are introduced in the radial continuation and in the gridding process. These are mitigated by iteration of the results and by choosing a data set that guarantees good spatial coverage (here: one month).

As a rule-of-thumb one could say that the expected geoid accuracy will be at the level of the orbit errors, provided sufficient velocity accuracy. From this error analysis one can expect an RSO-based geoid accuracy of a few dm, whereas RDO will lead to dm accuracy (and possibly sub-dm).

5 Results

Both with RSO and with RDO 3 monthly solutions were obtained: January, April and July 2002. As a main validation criterion we compare our results to EIGEN-1S, both spatially and spectrally.

Spatial domain. For each geoid solution the difference w.r.t. the EIGEN-1S geoid was taken and averaged over longitude in RMS sense. The resulting latitude RMS curves are displayed in fig. 5. The RSO results are clearly in the 2–3 dm accuracy range, although one curve (representing July) is clearly closer to EIGEN-1S than the others. This can either be coincidence or it could hint at time-changes in the gravity field. Because the XO calibration process hardly depends on the a priori gravity field, the error level is a reliable indicator of the quality of these RSO results.

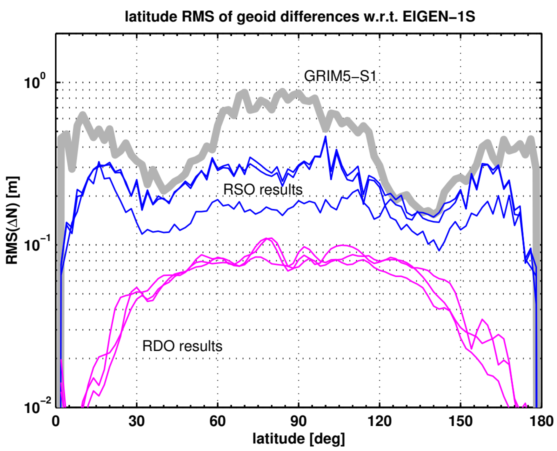

Fig. 5. Spatial RMS over latitude circles of geoid solutions w.r.t. EIGEN-1S. The gray curve represents the difference between EIGEN-1S its predecessor GRIM5-S1

The RDOs allow a recovery down to (or even below) 1 dm. All months are more or less equivalent. Of course this is not an absolute error measure but only a comparison to EIGEN-1S. It must be noted that the calibration process through 15-minute energy slope analysis does depend on the a priori gravity field far stronger than the XO-calibration. The RDO results are forced towards EIGEN-1S. The slope comparison effectively means that the *average* geoid slope in our solutions over 15-minute arcs—60° or about 7000 km—is taken from the a priori model. Recall that ground-tracks are basically North-South.

The above results are in line with the error analysis and expectations in the previous section.

Spectral domain. Figure 6 displays the results in the SH spectral domain in a condensed way. Degree RMS curves are displayed for the RSO and RDO geoid results—actually the difference w.r.t. EIGEN-1S again—in comparison to error spectra of EIGEN-1S and GRIM5-S1 and to signal spectra.

The RSO-July result is again significantly closer to EIGEN-1S than the January and April results. From fig. 6 we conclude that even RSO based geoid solutions are a great improvement over the pre-CHAMP model GRIM5-S1. The quality of the RDO results is

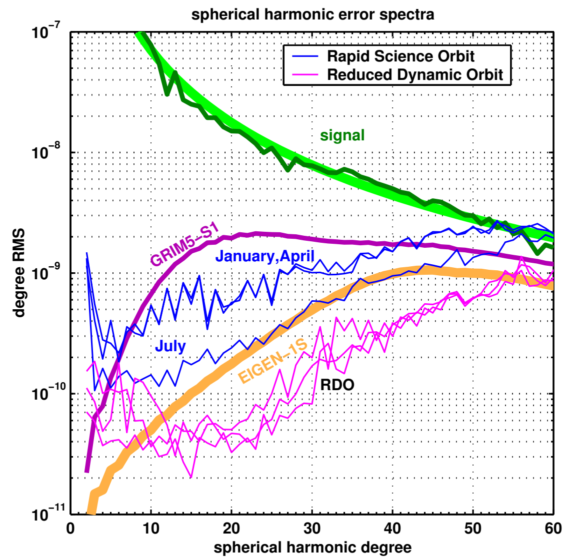

Fig. 6. Spectral RMS geoid solutions w.r.t. EIGEN-1S. For comparison, also EIGEN-1S signal and error spectra and the GRIM5-S1 error spectrum are shown. The RSO results are represented by the 3 wiggly curves between EIGEN-1S and GRIM5-S1. The RSO results are below the EIGEN-1S curve, except for the lowest degrees.

compatible with EIGEN-1S. Again, because of the dependence on the a priori model in the accelerometer process, the RDO error curve does not represent an absolute error level. It is merely an indication of the achievable accuracy.

Figure 5 also shows that the results in the lowest degrees ($l \leq 10$) are relatively poor. It is unclear what the main contributor to this phenomenon is: the accelerometer data in conjunction with the calibration process, or the energy balance approach itself. In any case, this situation does not favour the determination of long-wavelength gravity field changes over time. In an attempt to reveal time changes the RSO results have been smoothed with a cap radius of 30°. Figure 7 displays the corresponding geoids for April and July 2002. At this stage it is unclear whether the pattern is noise, unmodelled polar motion, or real time-variable gravity effects.

6 Conclusions

The energy integral approach offers several advantages over other gravity recovery methodologies. It is based on a relatively easy equation. Apart from the integration of the dissipative accelerations, all quantities used are in-situ. No orbital dynamics other than implied by the Jacobi-integral is involved. Thus no

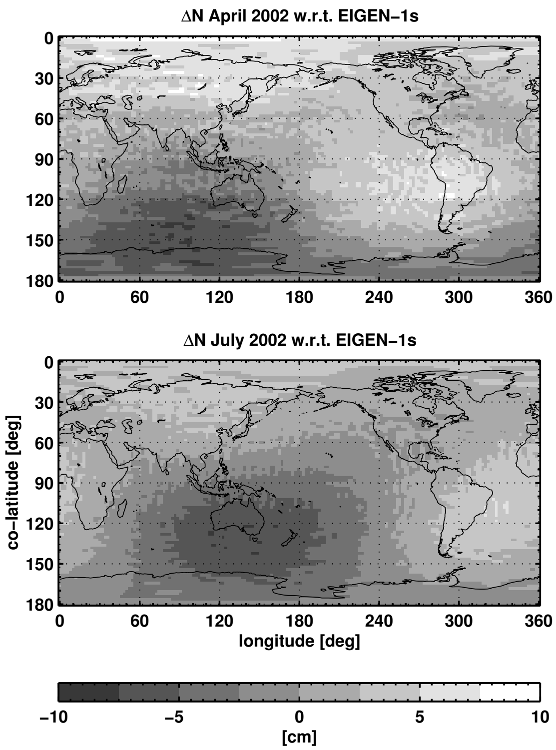

Fig. 7. Smoothed RSO results (cap radius of 30°).

numerical integration of equations of motion or of variational equations is required, there is no initial state problem, and there is no need for a combined inversion of orbit and gravity field parameters. One only needs orbital and accelerometer data.

The disturbing potential at satellite altitude can be estimated with an accuracy of a few $\mathrm{m}^2/\mathrm{s}^2$ using Rapid Science Orbits and even below $1\,\mathrm{m}^2/\mathrm{s}^2$ when precise Reduced Dynamic Orbits are used. Using Bruns's equation this roughly translates into a geoid accuracy of a few dm with RSO and potentially below 1 dm with RDO. In general, an error analysis of the Jacobi integral and of the data processing steps tells us that the geoid accuracy to be expected is roughly at the same level as the positional orbit errors, provided compatible velocity accuracy and good data distribution. The latter can be critical now and then, since CHAMP's decaying orbit causes it to go through certain repeat modes, during which the ground-track pattern is sparse.

The RSO accuracies do not allow for the resolution of time-variable gravity field. Energy integral based gravity recovery using RSO has a reduced sensitivity at the lowest degrees. The RDO-based monthly geoids are potentially of sufficient quality to uncover time variations in the gravity field. However, the present results have been forced towards EIGEN-1S too much by the calibration process. Thus, future research will have to optimize the calibration process for RDOs.

The cross-over analysis for calibrating the accelerometer data is an excellent technique to monitor the accelerometer's behaviour over time. It only weakly depends on a-priori gravity field information. It is therefore an independent measure of energy dissipation.

Acknowledgments Discussions with Prof. Manfred Schneider about the Jacobi integral, its derivation and its history are gratefully acknowledged. We thank GFZ Potsdam for the provision of CHAMP data.

References

Bjerhammar, A. (1967). *On the energy integral for satellites*. Technical report, The Royal Institute of Technology, Stockholm.

Gerlach, C., Sneeuw, N., Visser, P., & Švehla, D. (2002). CHAMP gravity field recovery with the energy balance approach: first results. Proceedings of the 1st CHAMP International Science Meeting, Potsdam, January 2002.

Han, S.-C., Jekeli, C., & Shum, C. K. (2002). Efficient gravity field recovery using in situ disturbing potential observables from CHAMP. *Geophys. Res. Letters*, in press.

Jekeli, C. (1999). The determination of gravitational potential differences from satellite-to-satellite tracking. *Cel. Mech. Dyn. Astron.*, 75, 85–101.

O'Keefe, J. A. (1957). An application of Jacobi's integral to the motion of an earth satellite. *The Astronomical Journal*, 62(1252), 265–266.

Reigber, C. (1969). *Zur Bestimmung des Gravitationsfeldes der Erde aus Satellitenbeobachtungen*. Reihe C 137, Deutsche Geodätische Kommission.

Reigber, C., Balmino, G., Schwintzer, P., Biancale, R., Bode, A., Lemoine, J.-M., Koenig, R., Loyer, S., Neumayer, H., Marty, J.-C., Barthelmes, F., Perosanz, F., & Zhu, S. (2002). A high-quality global gravity field model from CHAMP GPS tracking data and accelerometry (EIGEN-1S). *Geophys. Res. Letters*, 29(14). 10.1029/2002GL015064.

Schneider, M. (1992). *Grundlagen und Determinierung*, volume I of *Himmelsmechanik*. BI-Wissenschaftsverlag. In German.

Sneeuw, N. (2001). Satellite geodesy on the torus: Block-diagonality from a semi-analytical approach. In M. G. Sideris (Ed.), *Gravity, Geoid and Geodynamics*, volume 123 of *IAG Symposia* (pp. 137–142).: IAG Springer-Verlag. GGG2000, Banff, Canada.

Visser, P. N. A. M., Sneeuw, N., & Gerlach, C. (2002). Energy integral method for gravity field determination from satellite orbit coordinates. *J. Geodesy*, submitted.